

GISANS for advanced functional layers

Current global consumer challenges require low cost, environmentally friendly processes and novel materials for harvesting energy and optimizing life quality. Significant multidisciplinary interest has been growing for thin nm-sized layers applied as sustainable materials for: organic photovoltaics, hybrid organic-inorganic solar cells, perovskite solar cells, batteries, smart coatings based on polymer gels. Upon confinement to the nm-scale, the role of interfaces (air, solvent, substrate) and the enthalpic interactions between the materials can lead to different surface and internal morphology for thin films compared to bulk materials.¹

In nanotechnological fabrication of such thin films, different materials, quite often incompatible to each other, can be simultaneously present.² Bottom-up preparation protocols using solvent and thermal annealing have displaced optical methods (such as photolithography) due to the much higher cost of the latter method. Using such preparation protocols, one can tune the orientation of the nanoscopic domains along or across the surface. A common stringent quality criterion for success of the fabrication and the layer performance in e.g. organic photovoltaics, batteries, hybrid solar cells and responsive polymer hydrogel films is the exact control of both surface morphology and internal/sub-surface nanostructure in terms of sizes, orientations and spacings from domains and defects. Performance and stability of thin functional layers critically depends on their inner and buried morphology, preparation as well as post-processing conditions.

Neutrons have the advantage that they can penetrate significantly in materials. Small angle neutron scattering (SANS) operates in transmission mode and the intensity stems from interaction between incident neutrons and the atomic nuclei as in contrast to X-rays where the X-ray photon interacts with the free electron clouds of the atom. For soft matter research and applications where low atomic number materials are used, large contrast can be obtained by the large scattering length density difference between hydrogen and deuterium. In cases where the position of different components within a layer and the corresponding nanostructure has to be discriminated and these components exhibit no significant differences in X-ray scattering contrast, the use of deuterated macromolecules or deuterated solvent enables to maintain the neutron contrast high enough and to resolve these domains. In addition, neutrons, in contrast to X-ray photons, have a polarization and as such can interact with the nuclei of atoms, thus enabling magnetic studies to be performed, e.g. for studying the direction of magnetization vectors.

Classical real-space microscopic techniques such as atomic force microscopy (AFM) or scanning electron microscopy (SEM) are mandatory, as they allow to probe surface characteristics, such as surface RMS roughness and height variation. However, they are limited to film surfaces. For a complete understanding of the performance and nanostructure of such layers, nanoscale sub-surface information is required over a broad sample area. Ideally this investigation should be obtained with the least destructive way as possible, so that the sample is not distorted. Grazing Incidence Small Angle Neutron Scattering (GISANS) is an advanced metrological technique ideally suited for such investigations.

In order to characterize films, we systematically utilize GISANS, a powerful adaptation using reflection-geometry of typical elastic SANS for thin films. The angle of incidence (α_i) is very small ($\alpha_i < 0.5^\circ$) in order to maintain a large illumination area under reflection mode and hence a large scattering volume for the thin film geometry. The technique was first developed in the late 90's by Müller-Buschbaum and coworkers³⁻⁵ for probing changes in the morphology and

inner structure after dewetting of polymer blends under different annealing conditions and has recently been utilized more for various thin film investigations.^{1,4-5}

GISANS has a broad spatial resolution (1-300 nm) and allows to probe in a non-destructive and non-invasive manner the size of nanostructured domains, their orientation and size distribution, as well as correlations between these morphological features across the film and along the film's surface. GISANS operates in the inverse space domain and inspects a macroscopic sample area, thus enabling superior statistics at one shot, and allows to probe sub-surface morphological features, compared to AFM and SEM.

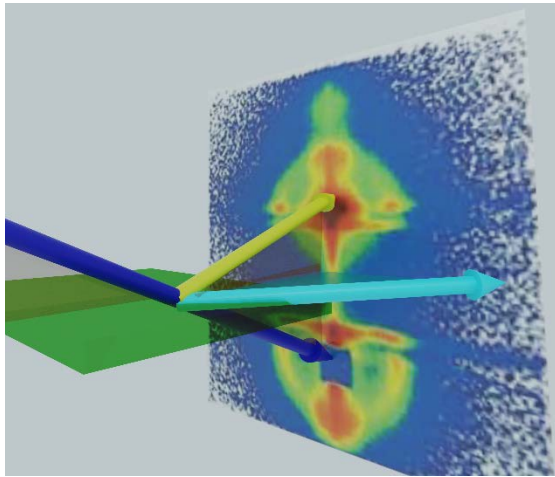


Figure 1. Schematic cartoon of the GISANS geometry. An incident neutron beam (dark blue arrow) impinges on the film (dark green) with incident angle α_i with respect to the film's surface. Upon hitting the film and neglecting absorption, transmission ($\alpha_t = -\alpha_i$), scattering and reflection ($\alpha_r = \alpha_i$) occurs. The parameter α_f (not shown) is the exit angle of the beam on the detector. The in-plane (cyan arrow) and out-of-plane (yellow arrow) scattering contributions are also shown. A GISANS pattern is finally obtained on the 2D detector. Adapted from: P. Müller-Buschbaum et al.⁷

As shown in Fig. 1, the incident neutron beam (blue) impinges on the sample surface (dark green) and the scattered signal (in-plane and out-of-plane scattering directions shown by the cyan and yellow arrow, respectively) is collected on a 2D detector, where a scattering pattern is obtained. These data are reduced to 1D data by performing horizontal (along sample's plane, red line in Fig.2a) and vertical (normal to the sample plane, dashed white line in Fig.2a) line integral cuts from which the in-plane correlated roughness and domain size spacing, as well as surface roughness and layer thickness can be obtained. Using fitting routines and simulations (e.g. BornAgain from JCMS Juelich) we typically model our experimental data with different appropriate form and structure factors. In this way, we can identify the exact shape and size of buried scattering domains as well as their interplanar spacing and spatial distribution.

Depending on the instrument settings, GISANS can be performed on either monochromatic (single wavelength, λ , with certain resolution $\Delta\lambda/\lambda$, with a neutron velocity selector) or polychromatic mode (broad range of λ using several choppers), depending on the experimental needs. The monochromatic mode offers higher neutron flux and better statistics. In the polychromatic mode, so-called time-of-flight GISANS (TOF-GISANS), a broad band of different neutron λ values can be used in the very same experiment (Fig. 2), allowing to (i) probe simultaneously different sub-sections of the whole film and (ii) to perform time-resolved experiments. The material's neutron scattering length density (ρ_{neutron}) expresses the strength of the atomic nuclei interaction with the impinging neutron. When $\alpha_f = \alpha_c$ (where α_c the critical angle of the material), the GISANS intensity is maximized due to standing waves formed in the material and thus to total external reflection, the so-called Yoneda peak. Considering⁷ that $\alpha_c(\lambda) = \lambda \cdot \sqrt{(\rho_{\text{neutron}}/\pi)}$, large λ allow to probe near-surface morphology ($\alpha_i < \alpha_c$) and small λ to probe more bulk information ($\alpha_i > \alpha_c$).

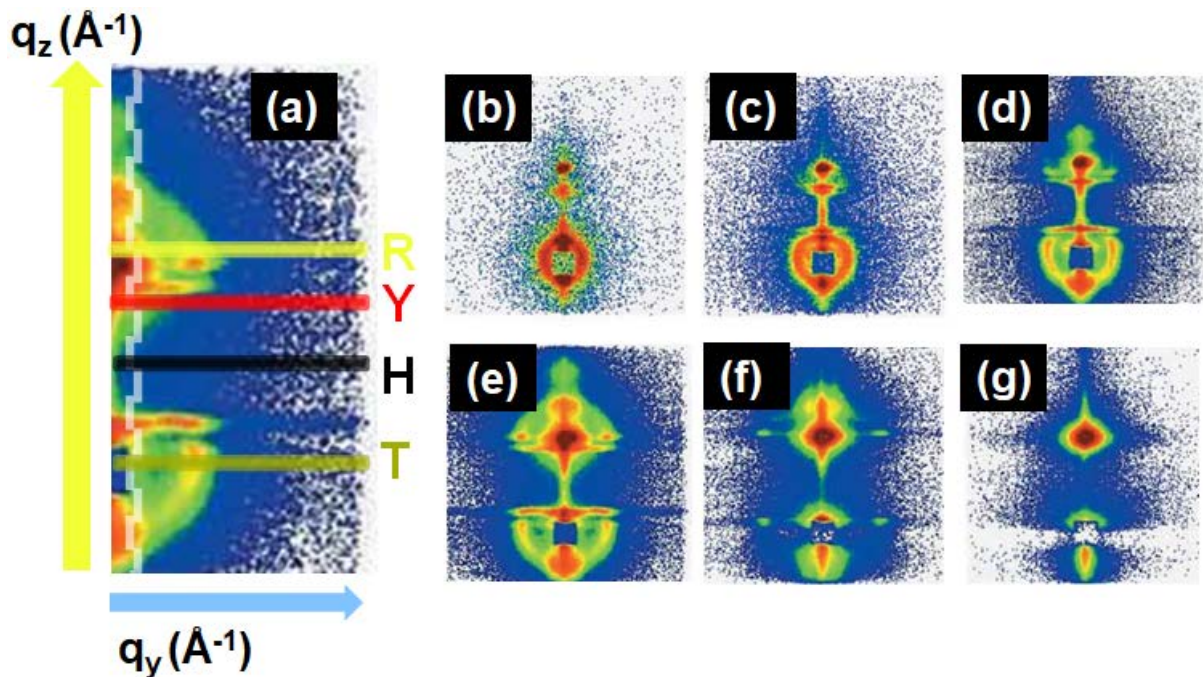


Figure 2. Panel (a) Schematic cartoon of a TOF-GISANS pattern on the 2D detector. The horizontal (cyan) and vertical (yellow) wavevectors (in \AA^{-1}), q_y and q_z , are drawn to guide the eye. The following features along q_z are also indicated: transmitted beam (T), sample horizon (H), Yoneda peak (Y) and reflected, or, specular peak (R). The $I(q_y)$ and $I(q_z)$ cuts are drawn by the red line and the dashed white line, respectively; panels (b) to (g): 2D TOF-GISANS patterns at different λ (\AA) and hence α_i , increasing from top-left to bottom-right as follows (λ) = 2.5, 3.3, 4.4, 5.8, 8.3 and 12.3. Adapted and redrawn from: P. Müller-Buschbaum et al.⁷.

The temporal resolution using TOF-GISANS is high enough that allows to monitor in-situ phenomena, such as the evolution of nanostructural changes in supported layers, such as during water ingress in mesoporous titania (TiO_2) films, or, water uptake during hydrogel swelling.

We highlight certain examples from GISANS studies in thin functional materials:

- **In the field of organic solar cells:**⁸ the exact nanostructure of the active layer in solar cells has crucial impact on the solar cell power conversion efficiency. We have successfully demonstrated using GISANS the length scales of phase separation and intermixing in bulk heterojunctions of P3HT:PCBM polymer blends, or, how post-processing with organic solvents⁹ can be used to optimize the domain sizes in the nm scale to achieve higher power conversion efficiencies.
- **Perovskite solar cells:** water uptake can be a challenge that deteriorates their performance. By exposing perovskite solar cells in D_2O ,¹⁰ we demonstrated a relation between chemical composition of the perovskite layer and its stability against water-induced degradation. Moreover, GISANS allowed us to develop a model which can describe the water incorporation of perovskite.
- **In hybrid organic/inorganic templates:** semiconductor oxides possess tremendous potential for photovoltaics, due to their well-defined nano/mesoporous structure. Their optimal use as templates in such photovoltaic applications depends on how efficient backfilling with solvents/conducting substances can be. We have identified a correlation between D_2O uptake and properties of the mesoporous TiO_2 nanostructure, including the elastic modulus and matrix deformation.^{11,12} Also, GISANS

allowed us to verify homogeneous distribution of nanostructure in mesoporous TiO₂ matrices across the layer¹³, or to correlate hybrid solar cell performance with TiO₂ nanostructure as template after filling with conducting polymers.¹⁴

- **In case of battery-related research:** GISANS was used to probe the porosity and TiO₂ intertubular distance in TiO₂ conductive matrices and correlate this to lithiation/delithiation efficiency.¹⁵⁻¹⁶ Moreover, GISANS showed preferential adsorption of iron oxide nanoparticles into deuterated polystyrene PSd domains from P(Sd-b-BMA) templates and this was accompanied by superparamagnetic behavior.¹⁷⁻¹⁸
- **Supported polymer gel layers/thermodynamics and substrate effects:** supported layers of block copolymers represent essential building blocks for soft robotics actuators and nanoswitches, as well as like hierarchical templates.¹⁹ Such films can be subject to external stimuli, such as temperature, pressure, pH, ionic strength and thus demonstrate deformability. GISANS has demonstrated how conformation of supported polymers can exhibit anisotropy due to the confinement,²⁰ the length scales of phase separation²¹ or near-surface and inner morphology in presence of defects⁷ in diblock copolymer films and the nanostructural rearrangement along the film's plane during water uptake/release.²²
- **Current directions:** Extreme environmental conditions (pressure, temperature, airflow, humidity) can have crucial impact on the final layer nanostructure and thus to performance as part of a functional device. This can be crucial for semiconductor oxide mesoporous templates, as well as swollen polymer thin films with pressure-dependent phase behavior. For instance, the role of pressure as intensive parameter in the phase behavior of supported swollen thin layers has scarcely been investigated. Our group has used GISANS to systematically investigate the impact of humidity and film responsiveness. We are currently extending already available multi-purpose sample environments that will allow us to monitor both structural rearrangements at the nano/mesoscale under the impact of such extreme conditions, together with some additional characterization tools in parallel (e.g. spectroscopy).

[1] A.Hexemer, P. Müller-Buschbaum (2015). *Advanced grazing incidence techniques for modern soft matter materials analysis (feature article)* IUCrJ 2, 106-125

[2] P.Müller-Buschbaum (2016). *GISAXS and GISANS as metrology technique for understanding the 3D morphology of block copolymer thin films*; Eur. Polym. J. 81, 470-493

[3] P. Müller-Buschbaum, J. S. Gutmann, M. Stamm (1999). *Dewetting of confined polymer films: An x-ray and neutron scattering study*; Phys. Chem. Chem. Phys. 1, 3857-3863

[4] P. Müller-Buschbaum, M. Wolkenhauer, O. Wunnicke, M. Stamm, R. & W. Petry. (2001). *Structure Formation in Two-Dimensionally Confined Diblock Copolymer Films*. Langmuir, 17(18), 5567–5575

[5] O. Wunnicke, P. Müller-Buschbaum, M. Wolkenhauer, C. Lorenz-Haas, R. Cubitt, V. Leiner, & M. Stamm (2003). *Stabilization of Thin Polymeric Bilayer Films on Top of Semiconductor Surfaces*. Langmuir, 19(20), 8511–8520

[4] P. Müller-Buschbaum (2013) *Grazing incidence small angle neutron scattering: Challenges and possibilities*; Polymer Journal (invited review) 45, 34-42

[5] S.Jaksch, T.Gutberlet, P.Müller-Buschbaum (2019). *Grazing incidence scattering – status and perspectives in soft matter and biophysics*. Curr. Opin. Colloid. Interface Sci. 42, 73-86

[7] P. Müller-Buschbaum, G. Kaune, M. Haese-Seiler, J.-F. Moulin (2014). *Morphology determination of defect-rich diblock copolymer films with time-of-flight grazing incidence small angle neutron scattering*. J. Appl. Cryst. 47, 1228-1237

[8] K. S. Wienhold, X. Jiang, P. Mueller-Buschbaum (2020), Appl. Phys. Lett., 116, 120504

[9] S. Guo, B. Cao, W. Wang, J.-F. Moulin, P. Müller-Buschbaum (2015). *Effect of alcohol treatment on the performance of PTB7:PC71BM bulk heterojunction solar cells*. ACS Appl. Mater. Interfaces 7, 4641-4649

[10] J. Schlipf, Y. Hu, S. Pratap, L. Bießmann, N. Hohn, L. Porcar, T. Bein, P. Docampo, P. Müller-Buschbaum (2019). *Shedding light on the moisture stability of 3D\2D hybrid perovskite heterojunction thin films*. ACS Appl. Energy Mater. 2, 1011-1018

- [11] L. Song, M. Rawolle, N. Hohn, J. S. Gutmann, H. Frielinghaus, P. Müller-Buschbaum (2018). *Deformation of mesoporous titania nanostructures in contact with D₂O vapor*. *Small* **14**, 18011461
- [12] L. Song, M. Rawolle, N. Hohn, J. S. Gutmann, H. Frielinghaus, P. Müller-Buschbaum (2019). *In situ monitoring mesoscopic deformation of nanostructured porous titania films caused by water ingress*. *ACS Appl. Mater. Interfaces* **11**, 32552-32558
- [13] G. Kaune, M. Haese-Seiler, R. Kampmann, J.-F. Moulin, Q. Zhong, P. Müller-Buschbaum (2010). *TOF-GISANS investigation of polymer infiltration in mesoporous TiO₂ films for photovoltaic applications*. *J. Poly. Sci. Part B*. **48**, 1628-1635
- [14] M. Rawolle, K. Sarkar, M. A. Niedermeier, M. Schindler, P. Lellig, J. S. Gutmann, J.-F. Moulin, M. Haese-Seiler, A. Wochnik, C. Scheu, P. Müller-Buschbaum (2013). *Infiltration of polymer hole-conductor into mesoporous titania structures for solid-state dye-sensitized solar cells*. *ACS Appl. Mater. Interfaces* **5**, 719-729
- [15] N. Paul, J. Brumbarov, A. Paul, Y. Chen, J.-F. Moulin, P. Müller-Buschbaum, J. Kunze-Liebhäuser, R. Gilles (2015). *GISAXS and TOF-GISANS studies on surface and depth morphology of self-organized TiO₂ nanotube arrays: model anode material in Li-ion batteries*. *J. Appl. Cryst.* **48**, 444-454
- [16] N. Paul, J. F. Moulin, G. Mangiapia, A. Kriele, P. Müller-Buschbaum, M. Opel, A. Paul (2020). *Surface distortion of Fe^{dor}-decorated TiO₂ nanotubular templates using time-of-flight grazing incidence small angle scattering*. *Sci. Rep.* **10**, 4038
- [17] Y. Yao, E. Metwalli, J.-F. Moulin, B. Su, M. Opel, P. Müller-Buschbaum (2014). *Self-assembly of diblock copolymer-maghemite nanoparticle hybrid thin films*. *ACS Appl. Mater. Interfaces* **6**, 18152-18162
- [18] Y. Yao, E. Metwalli, M. Opel, M. Haese, J.-F. Moulin, K. Rodewald, B. Rieger, P. Müller-Buschbaum (2016). *Lamellar diblock copolymer films with embedded maghemite nanoparticles*. *Adv. Mater. Interfaces* **3**, 1500712
- [19] C. J. Brett, N. Mittal, W. Ohm, M. Gensch, L. P. Kreuzer, V. Körstgens, M. Månsson, H. Frielinghaus, P. Müller-Buschbaum, L. D. Söderberg, S. V. Roth (2019). *Water-induced structural rearrangements on the nanoscale in ultrathin nanocellulose films*. *Macromolecules* **52**, 4721-4728
- [20] D. Magerl, M. Philipp, E. Metwalli, P. Gutfreund, X.-P. Qiu, F. M. Winnik, P. Müller-Buschbaum (2015). *Influence of confinement on the chain conformation of cyclic poly(N-Isopropylacrylamide)*. *ACS Macro Lett.* **4**, 1362-1365
- [21] P. Busch, M. Rauscher, J.-F. Moulin, P. Müller-Buschbaum (2011). *Debye-Scherrer rings from block copolymer films with powder-like order*. *J. Appl. Cryst.* **44**, 370-379
- [22] E. Metwalli, J.-F. Moulin, M. Rauscher, G. Kaune, M. A. Ruderer, U. van Bürck, M. Haese-Seiler, R. Kampmann, P. Müller-Buschbaum (2011). *Structural investigation of diblock copolymer thin films using TOF-GISANS*. *J. Appl. Cryst.* **44**, 84-92

